

# Caustic structures in the spectrum of x-ray Compton scattering off electrons driven by a short intense laser pulse

D. Seipt,<sup>1,\*</sup> A. Surzhykov,<sup>1</sup> S. Fritzsche,<sup>1,2</sup> and B. Kämpfer<sup>3,4</sup>

<sup>1</sup>*Helmholtz-Institut Jena, Fröbelstieg 3, 07743 Jena, Germany*

<sup>2</sup>*Universität Jena, Institut für Theoretische Physik, 07743 Jena, Germany*

<sup>3</sup>*Helmholtz-Zentrum Dresden-Rossendorf, Institute of Radiation Physics, P.O. Box 510119, 01314 Dresden, Germany*

<sup>4</sup>*TU Dresden, Institut für Theoretische Physik, 01062 Dresden, Germany*

We study the Compton scattering of x-rays off electrons that are driven by a relativistically intense short optical laser pulse. The frequency spectrum of the laser-assisted Compton radiation shows a broad plateau in the vicinity of the laser-free Compton line due to a nonlinear mixing between x-ray and laser photons. Special emphasis is placed on how the shape of the short assisting laser pulse affects the spectrum of the scattered x-rays. In particular, we observe sharp peak structures in the plateau region, whose number and locations are highly sensitive to the laser pulse shape. These structures are interpreted as spectral caustics by using a semiclassical analysis of the laser-assisted QED matrix element.

PACS numbers: 12.20.Ds, 32.80.Wr, 41.60.Cr

Keywords: laser-assisted Compton scattering, intense laser pulses, XFEL, caustic

X-ray free electron lasers (XFELs) help explore matter on ultra-short time-scales and under extreme conditions. Their high x-ray photon flux and short pulse duration of only a few femtoseconds allow to record transient processes like chemical reactions in real-time [1, 2]. Moreover, the x-ray scattering off dense plasmas—for instance those plasmas generated by irradiating a solid density target with an ultra-intense optical laser pulse [3]—facilitate the study of ultra-fast collective dynamics and plasma instabilities [4–7], which are important for novel particle acceleration [8–10] or fusion energy concepts [3], for instance.

Such extreme states of matter can be generated with the help of optical lasers that reached already intensities of  $10^{22}$  W/cm<sup>2</sup> [11]. The interaction of such laser pulses with electrons (with charge  $e$  and mass  $m$ ) is characterized by the laser’s normalized amplitude  $a_0 = |e|E_L/m\omega_L$ , where  $\omega_L$  and  $E_L$  are the frequency and amplitude of the laser electric field, respectively. Already for  $10^{18}$  W/cm<sup>2</sup> ( $a_0 \sim 1$ ), the electron’s quiver motion reaches relativistic velocities and its interaction with the laser’s magnetic field leads to a non-linear orbital motion, often denoted as “figure-8” [12]. At extreme light intensities,  $a_0 \gg 1$ , the electrons interact with many photons from the laser field simultaneously and one enters the realm of non-perturbative strong-field quantum electrodynamics (QED) [13–15].

High-intensity lasers can also be employed in laser-assisted scattering processes [16–31], where the presence of the strong low-frequency laser field modulates a hard QED scattering process. This could be, for instance, Compton scattering where a hard x-ray (or  $\gamma$ -ray) photon is scattered off a (quasi-)free electron with a frequency change that depends on the scattering angle [32]. The assisting strong low-frequency laser field leads to the formation of side-bands in the frequency spectrum close to

the laser-free Compton line, and already for  $a_0 \sim 1$  the electron interacts with a large number of laser photons [33].

In this letter, we present a QED description of laser assisted Compton scattering [33–38] of an ultra-short pulse of coherent x-rays from an XFEL off electrons moving in an intense ( $a_0 \sim 1$ ) and ultra-short synchronized optical laser pulse [39–41]. We analyze in detail the structures in the frequency spectrum of the scattered x-rays with regard to the influence of the specific shape of the assisting laser pulse and the ultra-fast laser-driven electron motion. By developing a semiclassical picture we identify the prominent peaks in the spectrum as *spectral caustics* emerging from coalescing stationary phase points where the quantum scattering amplitude is formed.

Caustics are a phenomenon known best from wave propagation. They occur when the rays associated to a wave field coalesce on a manifold of lower dimension, creating bright zones in the wave field. A well known example is the focal spot of a lens: All parallel light rays that impinge on the lens coalesce in a single point—the focal point. From the mathematical viewpoint, caustics are singularities of differentiable mappings [42, 43] and also occur in the spectral domain [44]. The notion of spectral caustics enables us to explain why the plateau region in the frequency spectrum is not flat, but has peaks at certain frequencies.

In our theoretical modeling of laser-assisted Compton scattering we describe the incident light of the XFEL ( $X$ ) and assisting laser ( $L$ ) as pulsed plane waves with frequencies  $\omega_{X,L}$  and durations  $T_{X,L}$ . They copropagate along the  $z$ -direction, described by the unit four-vector  $n^\mu = (1, 0, 0, 1)$ , with mutually orthogonal linear polarization four-vectors  $\varepsilon_{X,L}^\mu$ . These light pulses scatter off a free electron that has the four-momentum  $p^\mu$  prior to the interaction. We assume the x-rays to

be a *weak field* in the sense that just one x-ray photon interacts with the electron in a single scattering event [33]. The scattered x-ray photon has four-momentum  $k'^\mu = \omega' n'^\mu$ , with frequency  $\omega'$  and scattering direction  $n'^\mu = (1, \sin\vartheta \cos\varphi, \sin\vartheta \sin\varphi, \cos\vartheta)$ , where  $\vartheta$  is the scattering angle and  $\varphi$  denotes the azimuthal angle relative to the laser polarization direction. We employ units with  $\hbar = c = 1$  and the fine structure constant  $\alpha = e^2/4\pi$ . Scalar products between four-vectors are denoted as  $x \cdot p = x^0 p^0 - \mathbf{x} \cdot \mathbf{p}$ .

Given the above setting, and by employing Volkov states within the framework of strong-field QED in the Furry picture [13, 45], the frequency- and angle-differential cross section for laser-assisted Compton scattering can be expressed as [33]

$$\frac{d^2\sigma}{d\omega' d\Omega} = \frac{\alpha^2 \omega'}{4\pi \omega_L^2} \int_{-\infty}^{\infty} d\phi g_X^2(\phi) \frac{\langle |\mathcal{M}|^2 \rangle}{(n \cdot p)(n \cdot p - n \cdot k')}, \quad (1)$$

where  $g_X$  denotes the temporal envelope of the x-ray pulse. The squared scattering amplitude, for unpolarized electrons and unobserved polarization of the scattered x-rays, is given as a double-integral over the laser phase  $\phi = \omega_L(t - z)$ ,

$$\begin{aligned} \langle |\mathcal{M}|^2 \rangle &= \int d\phi d\phi' g_X(\phi) g_X(\phi') e^{i \int_{\phi'}^{\phi} d\phi'' \psi(\phi'', \ell)} \\ &\times \left( \eta - 2\alpha_X^2 - \frac{\alpha_X^2}{2} \eta [a_L(\phi) - a_L(\phi')]^2 \right), \quad (2) \end{aligned}$$

where  $a_L(\phi)$  denotes the laser's normalized vector potential and we abbreviate  $\eta = 2 + \frac{u^2}{1+u}$ ,  $u = \frac{n \cdot k'}{n \cdot p - n \cdot k'}$  and  $\alpha_X = \frac{m u}{\omega_X} \left( \frac{\varepsilon_X \cdot p}{n \cdot p} - \frac{\varepsilon_X \cdot k'}{n \cdot k'} \right)$ . The phase of the scattering amplitude (2) is determined by

$$\psi(\phi, \ell) = (\ell + \varkappa) \frac{n' \cdot v_L(\phi)}{n' \cdot v_0} - \varkappa, \quad (3)$$

where  $\varkappa = \omega_X/\omega_L$  denotes the ratio of the x-ray and assisting laser frequencies.

The quantity  $\ell$  describes the energy transfer from the laser field to the scattered x-ray photon and determines its frequency  $\omega'$  via nonlinear x-ray-optical frequency mixing [33, 46]:

$$\omega'(\ell) = \frac{(\omega_X + \ell \omega_L) n \cdot p}{p \cdot n' + (\omega_X + \ell \omega_L) n \cdot n'}. \quad (4)$$

The effective range of  $\ell$ , and hence also  $\omega'$ , can be quite large even for  $a_0 < 1$ , reaching values of  $\ell \sim a_0 \varkappa$  for large frequency ratios  $\varkappa$  [33].

Expression (3) that determines the phase of the scattering amplitude depends on the four-velocity of a classical electron moving in the laser field  $a_L^\mu(\phi)$ ,

$$v_L^\mu(\phi) = v_0^\mu - a_L^\mu(\phi) + n^\mu \frac{a_L(\phi) \cdot v_0}{n \cdot v_0} - n^\mu \frac{a_L^2(\phi)}{2n \cdot v_0}, \quad (5)$$

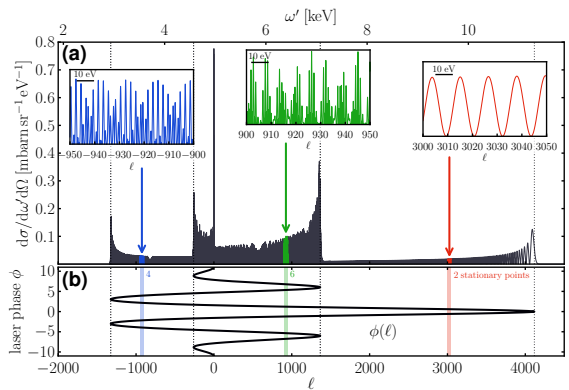


FIG. 1. Frequency spectrum of x-rays that are Compton scattered off laser-driven electrons (a) as a function of the scattered x-rays' frequency  $\omega'$  (upper axis) and the energy transfer  $\ell$  (lower axis). The initial x-ray pulse has a frequency of  $\omega_X = 5$  keV and a duration of  $T_X = 7$  fs. The assisting laser field that drives the electron-motion has peak amplitude  $a_0 = 1$ , frequency  $\omega_L = 1.55$  eV and pulse duration  $T_L = 5$  fs. The insets magnify the highly-oscillatory structure of the spectrum for three frequency ranges. Panel (b) depicts the function  $\phi(\ell)$  from inverting (6), which determines the number and positions of the stationary points for a given value of  $\ell$ . Spectral caustics appear at those  $\ell$  where the function  $\phi(\ell)$  has vertical tangents and two stationary points coalesce (vertical dotted lines).

where  $v_0^\mu = p^\mu/m$  is the electron's four-velocity before the laser pulse arrives. In Eq. (5), the terms linear in  $a_L$  describe the electron's quiver motion due to the laser electric field with frequency  $\omega_L$ . The  $a_L^2$ -term describes the interaction with the magnetic field and comprises both a longitudinal  $2\omega_L$  oscillation and a ponderomotive drift [12, 47, 48]. The superposition of the  $\omega_L$  and  $2\omega_L$  oscillations is often denoted as “figure-8” motion.

Figure 1 (a) displays the frequency spectrum of Compton scattered x-rays, Eq. (1), for a scattering angle of  $\vartheta = 45^\circ$  in the plane of the laser polarization,  $\varphi = 0$ . For convenience, from now on we work in the rest frame of the initial electron, where  $v_0^\mu = (1, 0, 0, 0)$ . We find a narrow large peak of laser-free Compton scattering at  $\ell = 0$ , which stems from x-ray photons that scatter outside the assisting laser pulse and, hence, with no energy exchanged between the electron and the laser field. Due to the action of the laser field and the frequency mixing (4) the spectrum has a broad structured plateau region between 3 keV and 11 keV with a number prominent large peak structures that we identify as spectral caustics below. In the regions between the caustics the spectrum is a highly oscillating function of  $\omega'$  on the scale of eV, as can be seen in the insets of Fig. 1 (a).

To gain an intuitive understanding for the complex peak structure in the spectrum in Fig. 1 and their relation to the laser-driven electron motion, Eq. (5), it is useful to resort to a semiclassical picture by applying a

stationary phase analysis [26, 49]. Because the integrand of (2) is a highly oscillating function of the laser phase  $\phi$  for large frequency ratios  $\varkappa = \omega_X/\omega_L \gg 1$  and  $a_0 \sim 1$ , the scattering amplitude, Eq. (2), is formed mainly at those laser phases that fulfill the stationarity condition  $\psi(\phi, \ell) = 0$ . Solving this implicit equation maps the scattering of x-ray photons at a certain moment  $\phi$  to one particular value of the energy transfer

$$\ell(\phi) = \varkappa \left( \frac{n' \cdot v_0}{n' \cdot v_L(\phi)} - 1 \right), \quad (6)$$

and, by means of Eq. (4), to one unique frequency  $\omega'(\phi)$ . The semiclassical analysis of the laser-assisted Compton scattering process facilitates the following interpretation: The laser-driven electron moves classically according to Eq. (5), up to the laser phase  $\phi$ , where the x-ray photon scatters off the electron. At the moment of scattering the electron has acquired the velocity  $v_L^\mu(\phi)$  due to its interaction with the assisting laser field. Because the x-ray photon now scatters off a relativistic electron, its frequency is Doppler shifted [32], and the Doppler shift  $\mathfrak{D}(\phi) = \frac{n' \cdot v_L(\phi)}{n \cdot v_0}$  depends on the angle between the scattering direction  $n'$  and the instantaneous electron velocity  $v_L^\mu(\phi)$  at the moment of scattering. With the help of  $\mathfrak{D}(\phi)$ , the instantaneous frequency of the scattered x-rays can be written as

$$\omega'(\phi) = \frac{\mathfrak{D}(\phi)\omega_X}{1 + \frac{n \cdot n'}{n \cdot p} \mathfrak{D}(\phi)\omega_X}. \quad (7)$$

Thus, in the semiclassical picture the broad plateau in the frequency spectrum in Fig. 1 is formed because the x-ray photons scatter off accelerated electrons with a variable Doppler factor.

The structures observed in the plateau-region of the spectrum in Fig. 1 can be explained by elaborating further the semiclassical picture of the laser-assisted QED scattering process. The semiclassical mapping (6), relates a moment of scattering  $\phi$  to a *unique energy transfer*  $\ell(\phi)$ . However, as seen from Fig. 1 (b), the inverse function  $\phi(\ell)$  is multiple-valued. Thus, the probability to observe a scattered x-ray photon with a particular frequency  $\omega'(\ell)$  is determined by multiple stationary points. The contributions to the squared scattering amplitude from different stationary phase points interfere and that leads to the highly oscillatory behavior of the frequency spectrum in Fig. 1. For instance, in the region around  $\ell \approx 3000$  two stationary points contribute to the scattering amplitude, leading to a cosine-like oscillation of the spectrum (right inset), while around  $\ell \approx 900$  (middle inset) a total of 6 stationary points are relevant providing a more complex structure with multiple oscillation periods.

All the large sharp peaks in the frequency spectrum are interpreted as spectral caustics: They occur at those values of  $\ell$  where two branches of  $\phi(\ell)$  merge, i.e. two stationary points coalesce, and the function  $\phi(\ell)$  has vertical tangents, see Fig. 1. This type singularities of the

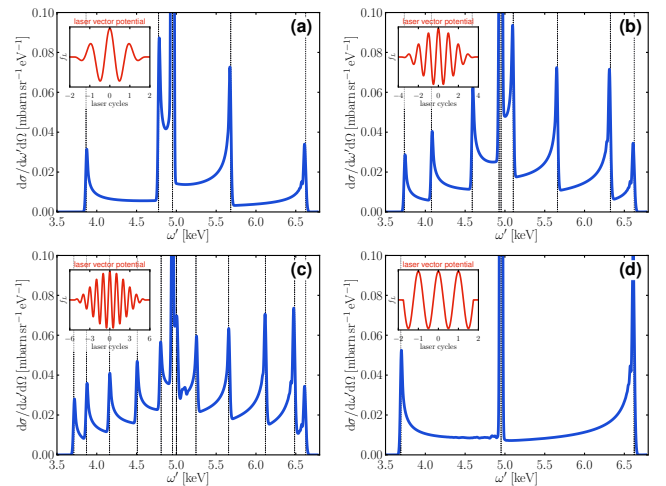


FIG. 2. The number and locations of the spectral caustic peaks in frequency spectrum of the scattered x-rays depends on both the shape and duration of the driving optical laser pulse (here with peak amplitude  $a_0 = 0.3$ ). The spectra are window-averaged (by a Gaussian with resolution 5 eV) to smooth the fast oscillations. Calculations are for a squared-cosine pulse with pulse durations  $T_L = 5$  fs (a), 10 fs (b) and 15 fs (c), and for a box shaped pulse with duration 9.34 fs (d). The vertical lines depict the calculated locations of the spectral caustics. The large laser-free Compton peak at  $\omega' = 4.95$  keV stems from the long x-ray pulse duration  $T_X = 25$  fs  $> T_L$ .

semiclassical mapping  $\phi(\ell)$  are spectral caustics of the fold-type  $A_2$ , with universal properties [43]. The universality allows to estimate the width of the spectral caustic peaks as  $\Delta\ell \sim (a_0\varkappa)^{2/3}$ , which is in good agreement with numerical calculations.

However, how can one understand the existence of the spectral caustic peaks from a physical viewpoint? The divergence of  $\phi(\ell)$  implies that the caustics are formed at those parts of the electron trajectory where the Doppler factor  $\mathfrak{D}(\phi_c)$  becomes stationary,  $\dot{\mathfrak{D}}(\phi_c) = 0$ , and the scattered x-rays have constant frequency over a long phase region. This generates a peak in the spectrum by “focusing” the scattered radiation to the spectral caustic peak at  $\omega'(\phi_c)$ . The stationarity of the Doppler factor implies that at the caustic formation phase  $\phi_c$  the four-acceleration of the electron is perpendicular to the scattering direction:  $n' \cdot \dot{v}_L(\phi_c) = 0$ .

Let us now calculate, within the semiclassical picture, the locations of the spectral caustic peaks in the frequency spectrum of the scattered x-rays and how they depend on the scattering direction  $n'$ . For that, we first have to solve the caustic condition  $n' \cdot \dot{v}_L(\phi_c) = 0$  for the phase  $\phi_c$  where the caustics are formed. Employing Eq. (5), we can write the caustic condition as

$$0 = \dot{f}_L(\phi_c) [a_0 f_L(\phi_c) - B(\vartheta, \varphi)], \quad (8)$$

with the laser pulse shape  $f_L$  and  $B(\vartheta, \varphi) =$

$\cos \varphi \sin \vartheta / (\cos \vartheta - 1)$ . Because Eq. (8) consists of the product of two terms we actually find two different classes of spectral caustics with distinct properties, which we denote as regular and irregular caustics, respectively.

The regular caustics follow from the solutions of  $\dot{f}_L(\phi_c) = 0$ . For laser pulses  $f_L = g_L \cos(\phi + \phi_0)$  with a slowly varying envelope  $g_L$ , with  $\dot{g}_L/g_L \ll 1$ , and the carrier envelope phase  $\phi_0$ , the caustics are formed at the phases  $\phi_c^{(n)} \approx n\pi - \phi_0$ ,  $n = 0, \pm 1, \dots$ . For ultra-short pulses, with  $\dot{g}_L/g_L \sim 1$ , the caustic formation phases  $\phi_c^{(n)}$  can be obtained numerically. The locations of the regular spectral caustics at  $\ell_{\text{reg}}^{(n)} = \ell(\phi_c^{(n)}) = \varkappa \xi^{(n)} / (1 - \xi^{(n)})$  with

$$\xi^{(n)} = (-1)^{n+1} a_0 g_L(\phi_c^{(n)}) \cos \varphi \sin \vartheta - \frac{a_0^2}{2} g_L^2(\phi_c^{(n)}) (1 - \cos \vartheta), \quad (9)$$

depend on the value of the laser vector potential  $a_L^\mu(\phi_c^{(n)})$  at its local extremal points, and, therefore, on the carrier envelope phase  $\phi_0$  and on the shape and duration of the pulse, see Fig. 2. The number of different spectral caustic peaks in the panels (a)–(c) grows with increasing laser pulse duration  $T_L$  for a smooth squared-cosine envelope  $g_L = \cos^2 \frac{\pi \phi}{2\omega_L T_L} \Theta(\omega_L T_L - |\phi|)$  with  $\Theta$  denoting the step-function. For a box-shaped envelope with a constant amplitude [Fig. 2 (d)] there are only two regular caustic peaks, irrespective of the pulse duration, because of  $g_L(\phi_c^{(n)}) = 1$ . Hence, in order to describe the peaks in the frequency spectrum correctly it is essential to exactly take into account the shape of the short laser pulse. To resolve the individual caustic peaks, their separation should be larger than their width  $\Delta \ell \sim (a_0 \varkappa)^{2/3}$ . This gives the order of magnitude estimate of the optimal laser pulse duration as  $\omega_L T_L \sim (a_0 \varkappa)^{1/3}$ .

The second type of caustics—the irregular caustics—occur where  $f_L(\phi_c) = B(\vartheta, \varphi)/a_0$  admits at least one real solution for  $\phi_c$ . In stark contrast to the regular caustics discussed above the location of the irregular caustic peak at  $\ell_{\text{irr}} = \varkappa \zeta / (1 - \zeta)$ , with  $\zeta = (1 - \cos \vartheta) B^2(\vartheta, \varphi) / 2$ , is independent of the laser pulse parameters. The irregular caustics are related to the longitudinal non-linear motion of the electrons due to the  $a_L^2$ -term in the classical electron velocity, Eq. (5). Therefore, they occur only for large enough scattering angles, e.g.  $\vartheta > 65^\circ$  in Fig. 3, where one probes dominantly longitudinal components of the electron velocity (5). This is related to the forward-backward asymmetry seen in Fig. 3 (a). The Doppler up-shift of the x-ray frequency for backward-scattering is limited by the longitudinal ponderomotive drift of the electron away from the observer. The existence of the irregular caustic peak in the spectrum signals the non-linear relativistic motion of the electrons, which comprises both the longitudinal ponderomotive drift and  $2\omega_L$  oscillations. In fact, the semiclassical mapping  $\ell(\phi)$ ,

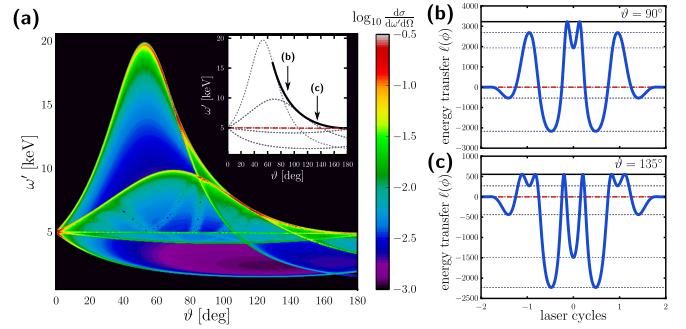


FIG. 3. The frequency- and angle-differential cross section for  $a_0 = 1.5$ , windowed by a Gaussian of 10 eV width (a). The pattern of the sharp peaks in the spectrum qualitatively coincides with the locations of the regular (gray dotted curves) and irregular (black solid curve) spectral caustics in the inset. The red dashed curve is the laser-free Compton line. Parameters are as in Fig. 1. In (b) and (c) the energy transfer  $\ell(\phi)$  oscillates with a frequency  $2\omega_L$  close to the irregular caustics. The horizontal lines have the same meaning as in the inset of panel (a).

Eq. (6), shows distinct  $2\omega_L$ -oscillations wherever the irregular caustics exist, see Fig. 3 (b,c).

Experiments on laser-assisted Compton scattering to verify the spectral caustic peaks in the spectrum could be done, e.g. at the future HIBEF beamline at the European XFEL [50] or the LCLS, with an XFEL pulse and an ultra-short intense optical laser pulse impinging simultaneously on an electron beam [33].

Due to the sensitivity of the locations of the spectral caustic on the laser pulse shape, the laser-assisted Compton scattering could give promise to measure the properties of relativistically intense laser pulses, in particular its peak amplitude  $a_0 \gtrsim 1$ , pulse duration and carrier envelope phase, for intensities exceeding the capabilities of atom-based schemes as stereo-ATI [51, 52].

The laser-assisted Compton scattering may be used to observe the dynamics of laser-driven electrons in more general situations, where the electrons are also subject to forces other than the laser field. The three-dimensional electron motion could be accessed by observing tomographically the frequency spectrum of Compton scattered x-rays for different scattering directions  $n'$ . For instance, this might be useful to investigate the complex laser-driven electron dynamics at the surface of a dense plasma, and could help to better understand the collisionless absorption of laser energy [53, 54], and its implications for plasma-based particle acceleration [55].

In summary, we study for the first time the details of the frequency spectrum of x-rays that are Compton scattered off an electron under the action of an intense *ultra-short* laser pulse. The rich pattern of large sharp peaks in the frequency spectrum is a novel feature that is related to the ultra-short duration of the assisting laser pulse, and is explained by means of a semiclassical pic-

ture as spectral caustics with universal properties. The notion of spectral caustics is a general one and could help understand also other laser-assisted scattering processes in ultra-short laser pulses.

---

\* d.seipt@gsi.de

- [1] Ph. Wernet *et al.*, “Orbital-specific mapping of the ligand exchange dynamics of Fe(CO)<sub>5</sub> in solution,” *Nature* **520**, 78 (2015).
- [2] M. P. Minitti *et al.*, “Imaging molecular motion: Femtosecond x-ray scattering of an electrocyclic chemical reaction,” *Phys. Rev. Lett.* **114**, 255501 (2015).
- [3] R. Kodama *et al.*, “Fast heating of ultrahigh-density plasma as a step towards laser fusion ignition,” *Nature* **412**, 798 (2001).
- [4] M. Marklund and P. K. Shukla, “Nonlinear collective effects in photon-photon and photon-plasma interactions,” *Rev. Mod. Phys.* **78**, 591 (2006).
- [5] S. H. Glenzer and R. Redmer, “X-ray thomson scattering in high energy density plasmas,” *Rev. Mod. Phys.* **81**, 1625 (2009).
- [6] R. Fäustlin *et al.*, “Observation of ultrafast nonequilibrium collective dynamics in warm dense hydrogen,” *Phys. Rev. Lett.* **104**, 125002 (2010).
- [7] T. Kluge, C. Gutt, L. G. Huang, J. Metzkes, U. Schramm, M. Bussmann, and T. E. Cowan, “Using x-ray free-electron lasers for probing of complex interaction dynamics of ultra-intense lasers with solid matter,” *Phys. Plasmas* **21**, 033110 (2014).
- [8] S. P. Hatchett *et al.*, “Electron, photon, and ion beams from the relativistic interaction of petawatt laser pulses with solid targets,” *Phys. Plasmas* **7**, 2076 (2000).
- [9] H. Schworer, S. Pfoth, O. Jäckel, K.-U. Amthor, B. Liesfeld, W. Ziegler, R. Sauerbrey, K. W. D. Ledingham, and T. Esirkepov, “Laser-plasma acceleration of quasi-monoenergetic protons from microstructured targets,” *Nature* **439**, 445 (2006).
- [10] J. Metzkes, T. Kluge, K. Zeil, M. Bussmann, S. D. Kraft, T. E. Cowan, and U. Schramm, “Experimental observation of transverse modulations in laser-driven proton beams,” *New J. Phys.* **16**, 023008 (2014).
- [11] V. Yanovsky *et al.*, “Ultra-high intensity- 300-TW laser at 0.1 Hz repetition rate,” *Opt. Express* **16**, 2109 (2008).
- [12] E. S. Sarachik and G. T. Schappert, “Classical theory of the scattering of intense laser radiation by free electrons,” *Phys. Rev. D* **1**, 2738 (1970).
- [13] V. I. Ritus, “Quantum effects of the interaction of elementary particles with an intense electromagnetic field,” *J. Sov. Laser Res.* **6**, 497 (1985).
- [14] F. Ehlotzky, K. Krajewska, and J. Z. Kamiński, “Fundamental processes of quantum electrodynamics in laser fields of relativistic power,” *Rep. Prog. Phys.* **72**, 046401 (2009).
- [15] A. Di Piazza, C. Müller, K. Z. Hatsagortsyan, and C. H. Keitel, “Extremely high-intensity laser interactions with fundamental quantum systems,” *Rev. Mod. Phys.* **84**, 1177 (2012).
- [16] V. P. Oleĭnik, “Resonance effects in the field of an intense laser beam,” *Sov. Phys. J. Exp. Theor. Phys.* **25**, 697 (1967).
- [17] E. Lötstedt, U. D. Jentschura, and C. H. Keitel, “Evaluation of laser-assisted Bremsstrahlung with Dirac-Volkov propagators,” *Phys. Rev. Lett.* **98**, 043002 (2007).
- [18] E. Lötstedt, U. D. Jentschura, and C. H. Keitel, “Laser channeling of Bethe-Heitler pairs,” *Phys. Rev. Lett.* **101**, 203001 (2008).
- [19] A. B. Voitkiv, N. Grün, and J. Ullrich, “Compton scattering of energetic photons by light atoms in the presence of a low-frequency electromagnetic field,” *J. Phys. B* **36**, 1907 (2003).
- [20] C. Müller, A. B. Voitkiv, and B. Najjari, “Relativistic electron-ion recombination in the presence of an intense laser field,” *J. Phys. B* **42**, 221001 (2009).
- [21] S. Schnez, E. Lötstedt, U. D. Jentschura, and C. H. Keitel, “Laser-assisted bremsstrahlung for circular and linear polarization,” *Phys. Rev. A* **75**, 053412 (2007).
- [22] K. Krajewska, “Electron-positron pair creation and Oleĭnik resonances,” *Laser Phys.* **21**, 1275 (2011).
- [23] A. Dadi and C. Müller, “Laser-assisted nuclear photoeffect,” *Phys. Rev. C* **85**, 064604 (2012).
- [24] C. Szymanowski, V. Vénier, R. Taïeb, and A. Maquet, “Mott scattering in strong laser fields,” *Phys. Rev. A* **56**, 3846 (1997).
- [25] S.-M. Li, J. Berakdar, J. Chen, and Z.-F. Zhou, “Laser-assisted mott scattering in the coulomb approximation,” *J. Phys. B* **37**, 653 (2004).
- [26] S. Meuren, K. Z. Hatsagortsyan, C. H. Keitel, and Antonino Di Piazza, “High-energy recollision processes of laser-generated electron-positron pairs,” *Phys. Rev. Lett.* **114**, 143201 (2015), arXiv:1407.0188.
- [27] S. J. Müller, C. H. Keitel, and C. Müller, “Particle production reactions in laser-boosted lepton collisions,” *Phys. Rev. D* **90**, 094008 (2014).
- [28] J. M. Ngoko Djiokap, H. M. Tetchou Nganso, and M. G. Kwato Njock, “Effects of the electron’s anomaly in relativistic laser-assisted mott scattering,” *Physica Scripta* **75**, 726 (2007).
- [29] R. Kanya, Y. Morimoto, and K. Yamanouchi, “Observation of laser-assisted electron-atom scattering in femtosecond intense laser fields,” *Phys. Rev. Lett.* **105**, 123202 (2010).
- [30] M. Boca, “Mott scattering of a klein-gordon particle in an intense laser field,” *Cent. Eur. J. Phys.* **11**, 1123 (2013).
- [31] S. P. Roshchupkin, “Resonant effects in collisions of relativistic electrons in the field of a light wave,” *Laser Phys.* **6**, 837–858 (1996).
- [32] A. H. Compton, “A quantum theory of the scattering of x-rays by light elements,” *Phys. Rev.* **21**, 483 (1923).
- [33] D. Seipt and B. Kämpfer, “Laser-assisted compton scattering of x-ray photons,” *Phys. Rev. A* **89**, 023433 (2014).
- [34] V. P. Oleĭnik, “Resonance effects in the field of an intense laser ray ii,” *Sov. Phys. J. Exp. Theor. Phys.* **26**, 1132 (1968).
- [35] R. Guccione-Gush and H. P. Gush, “Photon emission by an electron in a bichromatic field,” *Phys. Rev. D* **12**, 404 (1975).
- [36] A. I. Akhiezer and N. P. Merenkov, “Scattering of a photon by an electron moving in the field of a plane periodic electromagnetic wave,” *Sov. Phys. J. Exp. Theor. Phys.* **61**, 41 (1985), [*Zh. Eksp. Teor. Fiz.* **88**, 72 (1985)].
- [37] F. Ehlotzky, “Scattering of x-rays by relativistic electrons in a strong laser field,” *J. Phys. B* **22**, 601 (1989).
- [38] V. N. Nedoreshta, A. I. Voroshilo, and S. P. Roshchupkin, “Resonant scattering of a photon by an electron in

- the moderately-strong-pulsed laser field,” *Phys. Rev. A* **88**, 052109 (2013).
- [39] F. Tavella, N. Stojanovic, G. Geloni, and M. Gensch, “Few-femtosecond timing at fourth-generation x-ray light sources,” *Nature Photon.* **5**, 162 (2011).
- [40] N. Hartmann *et al.*, “Sub-femtosecond precision measurement of relative x-ray arrival time for free-electron lasers,” *Nature Photon.* **8**, 706 (2014).
- [41] S. Schulz *et al.*, “Femtosecond all-optical synchronization of an x-ray free-electron laser,” *Nature Commun.* **6**, 5938 (2015).
- [42] M. V. Berry and C. Upstill, “Catastrophe optics: Morphologies of caustics and their diffraction patterns,” in *Progress in Optics*, 18 (1980) p. 257.
- [43] Yu. A. Kravtsov and Yu. I. Orolov, “Caustics, catastrophes, and wave fields,” *Sov. Phys. Usp.* **26**, 1083 (1983).
- [44] O. Raz, O. Pedatzur, B. D. Bruner, and N. Dudovich, “Spectral caustics in attosecond science,” *Nature Photon.* **6**, 170 (2012).
- [45] D. M. Volkov, “Über eine Klasse von Lösungen der Diracschen Gleichung,” *Z. Phys.* **94**, 250 (1935).
- [46] T. E. Glover *et al.*, “X-ray and optical wave mixing,” *Nature* **488**, 603 (2012).
- [47] H. R. Reiss, “The mass shell of strong-field quantum electrodynamics,” *Phys. Rev. A* **89**, 022116 (2014).
- [48] D. Seipt, S. G. Rykovanov, A. Surzhykov, and S. Fritzsche, “Narrowband inverse Compton scattering x-ray sources at high laser intensities,” *Phys. Rev. A* **91**, 033402 (2015).
- [49] J. Z. Kamiński and F. Ehlötzky, “Generation of attosecond pulses in electron-ion recombination processes,” *J. Mod. Opt.* **53**, 7 (2006).
- [50] T. E. Cowan and the HIBEF collaboration, “Status of the proposed Helmholtz International Beamline for Extreme Fields (HIBEF) at the European XFEL,” (2013), APS Division of Plasma Physics Meeting 2013, abstract NP8.063.
- [51] G. G. Paulus, F. Grasbon, H. Walther, P. Villoresi, M. Nisoli, S. Stagira, E. Priori, and S. De Silvestri, “Absolute-phase phenomena in photoionization with few-cycle laser pulses,” *Nature* **414**, 182 (2001).
- [52] T. Wittmann, B. Horvath, W. Helml, M. G. Schätzel, X. Gu, A. L. Cavalieri, G. G. Paulus, and R. Kienberger, “Single-shot carrier-envelope phase measurement of few-cycle laser pulses,” *Nature Phys.* **5**, 357 (2009).
- [53] F. Brunel, “Not-so-resonant, resonant absorption,” *Phys. Rev. Lett.* **59**, 52 (1987).
- [54] P. Mulser, S. M. Weng, and T. Liseykina, “Analysis of the Brunel model and resulting hot electron spectra,” *Phys. Plasmas* **19**, 043301 (2012).
- [55] M. Veltcheva, A. Borot, C. Thauray, A. Malvache, E. Lefebvre, A. Flacco, R. Lopez-Martens, and V. Malka, “Brunel-dominated proton acceleration with a few-cycle laser pulse,” *Phys. Rev. Lett.* **108**, 075004 (2012).